PAPER • OPEN ACCESS

Laser-induced extreme magnetic field in nanorod targets

To cite this article: Zsolt Lécz and Alexander Andreev 2018 *New J. Phys.* **20** 033010

IOP Publishing New J. Phys. 20 (2018) 033010 https://doi.org/10.1088/1367-2630/aaaff2

New Journal of Physics
The open access journal at the forefront of physics

Deutsche Physikalische Gesellschaft DPG
IOP Institute of Physics

Published in partnership with: Deutsche Physikalische Gesellschaft and the Institute of Physics

OPEN ACCESS

RECEIVED
30 October 2017

REVISED
15 January 2018

ACCEPTED FOR PUBLICATION
16 February 2018

PUBLISHED
26 March 2018

PAPER

Laser-induced extreme magnetic field in nanorod targets

Zsolt Lécz[1] **and Alexander Andreev**[1,2]

[1] ELI-ALPS, ELI-HU Nonprofit Ltd., Szeged, Csongrad, Hungary
[2] Max-Born-Institut fur Nichtlineare Optik und Kurzzeitspektroskopie Berlin, Berlin, DE, Germany

E-mail: zsolt.lecz@eli-alps.hu

Keywords: high current, strong magnetic fields, laser-matter interaction, numerical simulations

Abstract

The application of nano-structured target surfaces in laser-solid interaction has attracted significant attention in the last few years. Their ability to absorb significantly more laser energy promises a possible route for advancing the currently established laser ion acceleration concepts. However, it is crucial to have a better understanding of field evolution and electron dynamics during laser-matter interactions before the employment of such exotic targets. This paper focuses on the magnetic field generation in nano-forest targets consisting of parallel nanorods grown on plane surfaces. A general scaling law for the self-generated quasi-static magnetic field amplitude is given and it is shown that amplitudes up to 1 MT field are achievable with current technology. Analytical results are supported by three-dimensional particle-in-cell simulations. Non-parallel arrangements of nanorods has also been considered which result in the generation of donut-shaped azimuthal magnetic fields in a larger volume.

1. Introduction

The reproduction of extreme conditions observed in stars or in interstellar media has always been a strong motivation for plasma physics community to develop techniques and concepts which can access astrophysical phenomena in laboratory environment. One of the most important and demanded quantity is a magnetic field in excess of a kiloTesla. The only source capable of generating such an ultra high magnetic field from laser-matter interactions is the return current of electrons flowing in the skin layer of plasma surfaces. This has been exploited to generate mega gauss magnetic fields on macroscopic scale [1, 2] or in laser-plasma interactions near the laser focal spot [3–5]. A single nanorod has been predicted to be able to induce an even gigagauss magnetic field. This leads to pinching of a cylindrical target [6]. This paper uses the same concept but is applied to multiple nanorods arranged in a uniform 2D array on a flat target surface.

There are several advantages in using nanorods arrays with intense laser pulses which arise from the high energy absorption efficiency [7, 8]. Such targets have been used in high energy density matter physics [6, 9, 10] and in generation of intense x-ray sources via laser-induced synchrotron radiation [11, 12]. Their usage, however, has not been considered, in detail, for the generation of extreme magnetic fields for applications or experiments. Here, a theoretical description of magnetic field generation by current densities existing in the nanorods interacting with intense laser pulses is presented. This work proposes target parameters and geometries to produce MT magnetic fields using laser pulses currently available in laboratory. The targets considered in this work and the direction of coordinate axes are shown in figure 1. In the case of standard parallel rods, the generated azimuthal magnetic fields are separated and limited near the individual nano-rods, in which a return current is flowing (red arrows). A reduction in the distance between the magnetic vortexes decreases the fields, but at the same time electron currents start to attract each other creating one return current near the axis of laser propagation. An extended azimuthal field distribution develops in a larger volume around the converging nanorods. These findings are supported by a 3D self-consistent particle-in-cell simulation which show good agreement with analytical modeling.

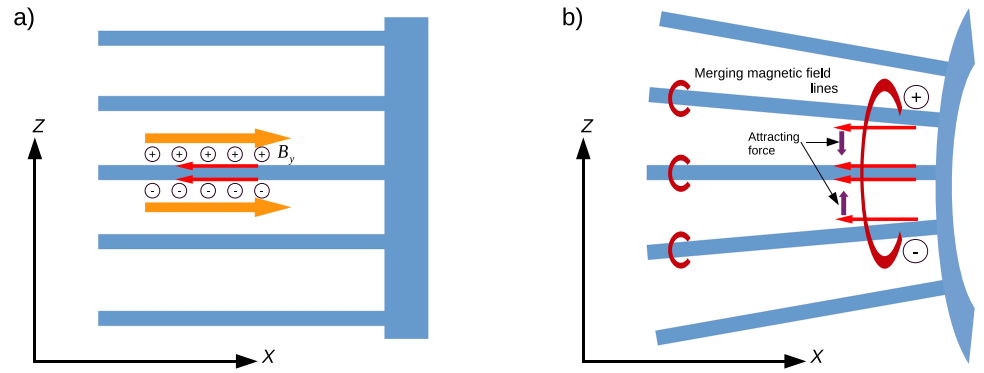

Figure 1. Schematic diagrams presenting the simulation setups for the two nanorod configurations: (a) parallel and (b) converging. The plus and minus signs show the direction of y component of the magnetic field, which is perpendicular to the plane of the drawing. The laser pulse propagates from the left boundary to the right.

2. Theory and modeling

In overcritical density plasmas, the flow of fast electrons generate a strong longitudinal current, which can reach the Alfén limit [13] and thus the self-generated magnetic field prevents these electrons from penetrating deep into the bulk material. Even if the current density is not that high, the parasitic Weibel instability causes strong filaments [14], in which the current density increases, leading to transversal spreading of hot electrons. In the case of thin nanorods (~100 nm in diameter), the return current (I_r) is spatially limited to the cross section of the rods, and exceeds the Alfén current [6, 15] without disturbing the fast electron propagation between the nanorods. The azimuthal magnetic field has a guiding role [12] and Weibel instability can not develop because its amplitude is much higher than the magnetic field induced by hot electrons. Two interaction regimes with different magnetic field distribution and its generation mechanisms can be distinguished and they depend on the target density and laser intensity.

2.1. Light nanorods

The laser intensity (I_L) is assumed to be high enough (or target density (n_0) is sufficiently low) so that all electrons within one laser wavelength are removed from the nanorods and are accelerated longitudinally by the laser field in vacuum between the nanorods. This can happen if the nanorod diameter is less or equal to the critical thickness, $2r_w \leqslant d_{\rm cr} = a_0(n_{\rm cr}/n_0)\,\lambda_L/\pi$ [16, 17], where $a_0 = eE_L/(m_e\omega_L c)$ is the normalized laser field amplitude and $n_{\rm cr} = \omega_L^2 m_e \epsilon_0/e^2$ is the critical density. The transversally extracted electrons can leave the nanorod at a maximum distance $r_e = a_0 c/\omega_L$ and thus the hot electron current can be expressed as $I_h = en_h v_h \pi r_e^2$, where $v_h \approx \kappa c$, with $0 < \kappa < 1$, is the average longitudinal velocity of hot electrons normalized to the speed of light and their density is estimated by using the fact that $I_h = I_r$, thus $n_h \approx n_0 r_w^2/(r_w + r_e)^2$. Assuming that $r_e \gg r_w$ leads to the expression $I_h \approx (\pi/2) en_0 r_w^2 c$; the magnetic field is calculated using $B_s = \mu_0 I_h/2\pi r_w$ leading to the following formula for the self magnetic field generated around the nanorods:

$$B_s^{\rm light} = \kappa \frac{\mu_0}{2} en_0 r_w c. \tag{1}$$

The maximum longitudinal extension of the azimuthal B-field is limited to one laser period. Beyond this region, no return current can exist and the remaining ions undergo Coulomb explosion. In order to maximize the magnetic field in this regime, the optimal case, $r_w = d_{\rm cr}/2$, is considered. This yields a peak amplitude: $B_s = \kappa E_L/2c = kB_L/2$ and shows that the maximum B-field achievable in the light rod regime is proportional to the laser magnetic field. The maximum field is actually $B_L/2$ in the case of high laser intensities when $\kappa \approx 1$ can be assumed.

2.2. Heavy nanorods

When rods have a diameter greater than the critical thickness, the removal of electrons continues over many laser periods and the maximum return current is limited by the target density and laser intensity. The number of electrons extracted from the target during one laser cycle can be approximated by $N_{\rm ex} = n_0 l_s \pi r_w^2$, where $l_s = \sqrt{a_0}\,c/\omega_p$ is the laser skin depth with $\omega_p = (e^2 n_0/m_e\epsilon_0)^{1/2}$ the plasma frequency. Assuming that the positive charge created on the tip of the rod can be neutralized within a half laser cycle, the cold electron current can be expressed as $I_r = 2eN_{\rm ex}/T_L = en_0 l_s r_w^2 \omega_L$, where T_L is the laser period. This current value is acquired during one laser cycle and continuously increases until the radial self electric field becomes equal to the laser

electric field. The maximum number of laser cycles (N_c) contributing to the build-up of the current density is 2π, obtained from the solution of $E_s = en'l_s/\epsilon_0 = E_L$, where $n' = N_c N_{\rm ex}/(\lambda_L \pi r_w^2)$ is the positive charge density in the nanorod. Obviously the number of periods in the laser pulse has to be higher than N_c in order to achieve the maximum field. Substituting this into the magnetic field formula results in $B_s = \mu_0 ecn_0(r_w/\lambda_L)l_s N_c = \mu_0 ecr_w\sqrt{n_0 n_{\rm cr} a_0}$, which can be written as

$$B_s^{\rm heavy} = 2\pi B_L \frac{r_w}{\lambda_L}\sqrt{\frac{n_0}{a_0 n_{\rm cr}}}. \tag{2}$$

This shows that the magnetic field scales with the target density as $B_s \sim n_0^{1/2}$ and only weakly depends on the laser intensity, $B_s \sim I_L^{1/4}$. Comparing equations (1) and (2) shows that there is a better scaling of the magnetic field with the laser and target parameters for light rods, but the plasma density is lower and thus the generated B-field is weaker in that regime. A larger radius of nanorods also increases the magnetic field, but it still must be much smaller than the laser wavelength otherwise a significant component of the laser wave would be reflected, greatly decreasing the efficiency of the process.

The definition of effective critical thickness [12] can be used in both regimes to express the self magnetic field in terms of $R = 2r_w/d_{\rm cr}$, which leads to the following function

$$B_s = \begin{cases} \kappa B_L R/2 = \kappa\omega_L^2 \frac{m_e}{2e}\frac{r_w}{c}\frac{n_0}{n_{\rm cr}} & \text{if } R \leqslant 1 \\ B_L\sqrt{R\omega_L r_w/c} = \omega_L^2 \frac{m_e}{e}\frac{r_w}{c}\sqrt{a_0\frac{n_0}{n_{\rm cr}}} & \text{if } R > 1. \end{cases} \tag{3}$$

A series of simulations measuring the azimuthal magnetic field from a single nanorod interacting with an intense field have been performed in order to check the reliability of results and to explore the transition between these regimes. The experimental conditions for $R \to \infty$ can be achieved by decreasing a_0 or by increasing n_0, which means that infinite magnetic field could be generated by using the right parameters. The simulations show that $B_s \to B_L$ if $R \to \infty$, the consequence of the limited penetration of the laser field into the plasma. So far, it has been assumed that the electrons are extracted from the whole cross-section of the nanorod, but in the case of high electron density, the laser field can extract electrons only from edge of the plasma (skin layer) and the number of extracted electrons will be $N_{\rm ex} = n_0\pi[r_w^2 - (r_w - l_s)^2]l_s \approx n_0\pi r_w l_s^2$, where the l_s^2 term is neglected because $l_s \ll r_w$. The resultant current is then $I_r = N_c\omega_L r_w a_0 c^2/\omega_p^2$, which results in a magnetic field:

$$B_s = B_L, \quad \text{if } R \to \infty. \tag{4}$$

3. 3D PIC simulations

The presented results were produced with the plasma simulation code VSim [18]. The grid cell size was always set to be equal to the half of the plasma skin depth (l_s) in order to correctly resolve the cold electron current inside the nanorods. The simulation box volume is $20 \times 3 \times 3 \times \mu{\rm m}^3$ and contains 9 nanorods at equal distances with radius of $r_w = 45$ nm. The laser pulse has a Gaussian longitudinal envelope with FWHM pulse duration $t_L = 30$ fs. A single nanorod has been used, with a subsequence reduction in transversal simulation domain size to 1 μm in order to verify the presented scalings and several simulations were performed in both regimes. After presenting the scaling of self-generated magnetic field, two standard cases with parallel and converging arrangement of nanorods will be discussed.

3.1. Single nanorod

Figure 2 shows two extreme cases, $R = 0.9$ and $R = 18$, and the difference between the two regimes are very clear. The laser pulse contains the z component of the magnetic field, thus the y component only originates from the self-field of the plasma. The longitudinal extension of the current density is very short, approximately $\lambda_L/2$, in the case of the light rod and the magnetic field is generated in this small volume. Behind this region, only ions are present which are practically immobile during a half laser period. In the case of a heavy rod, the laser field can not extract all electrons in one laser cycle but complete removal happens over several cycles. This can be seen in the current density distribution at $t = 40$ fs (figure 2(g)), which exhibits a bunched structure with 5 small bunches and then drops to zero. After a few laser cycles the current flows inside of the nanorod and not in the thin skin layer. The temporal evolution of the magnetic field is constant within the light rod regime but increases in time, up to the maximum value, in the case of the heavy rod. The return current partially neutralizes the highly positively charged part, which results in the reduction of the radial electric field and electron extraction can continue for the duration of the pulse. It means that the spatial extension of the magnetic field is limited by the pulse duration in this regime but its peak value is defined by the electron density.

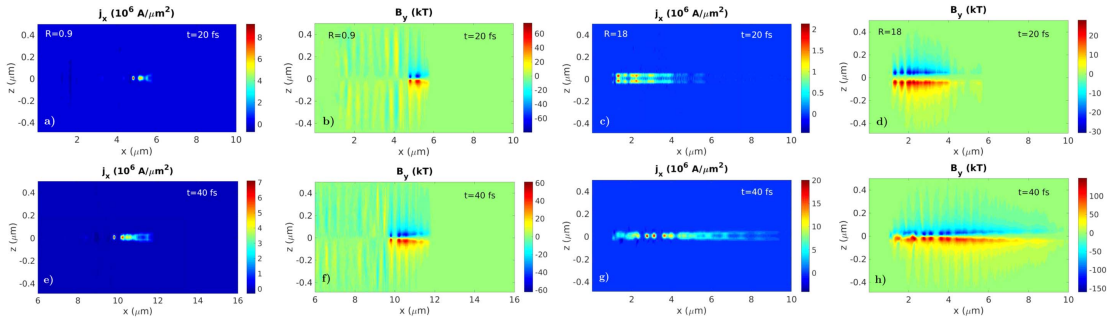

Figure 2. Longitudinal current density cross sections and distribution of the magnetic field perpendicular to the plane at different time instances from the light rod ($a_0 = 48$, $n_0 = 60n_{cr}$: (a), (b), (e), (f)) and heavy rod ($a_0 = 4.8$, $n_0 = 120n_{cr}$: (c), (d), (g), (h)) regimes.

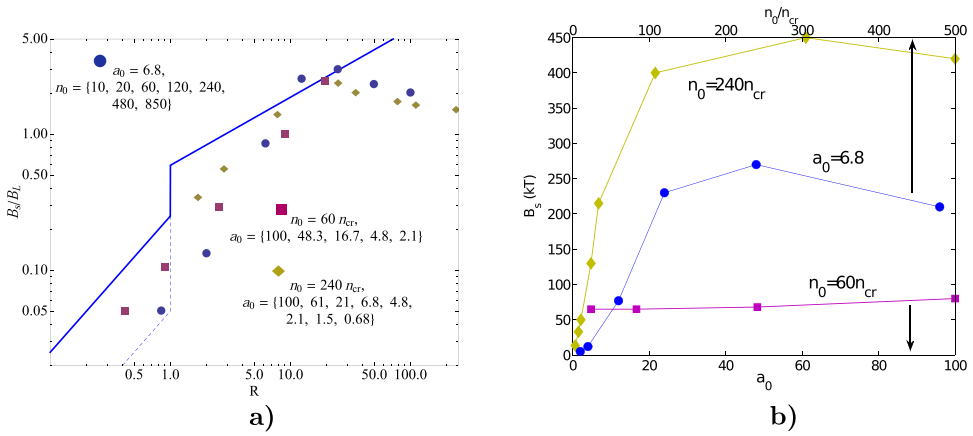

Figure 3. (a) Comparison of the analytical scaling given by equation (3) with the simulation results. The solid line is with $\kappa = 0.5$ and the dashed with $\kappa = 0.1$. The order of the values in the brackets is the same as order of the discrete points. (b) The dependence of the same magnetic field amplitudes as a function of laser field and plasma density.

A brief parameter-scan has been performed in the case of the nanorod shown above and the measured maximum values of B_y are shown in figure 3(a). The continuous and dashed lines correspond to equation (3) but the data is taken from simulations where either the plasma density or laser intensity is kept constant. There is no observable jump in the B-field over the transition zone between the two regimes but the trends in the results for $R \ll 1$ and $R \gg 1$ are very similar to the analytical findings. The data points in the transient regime fit very well with the scaling function $\sim R^{\eta}$, where $1 < \eta < 1.5$. Figure 3(b) shows the absolute values of the B-field as functions of n_0 and a_0, confirming that the B-field scales with the square of laser amplitude in one regime ($R > 1$, yellow line) and is independent of the laser intensity in the other regime ($R < 1$, purple line). The $\sim\sqrt{n_0}$ scaling is also shown in the case of heavy nanorods (the blue line in figure 3(b)).

A simulation with a super heavy nanorod is presented in figure 4. In this case, the return current is located near the edge of the plasma and is extended up to the plasma skin depth. The magnetic field resembles the shape of the laser pulse envelope. The longitudinal extension of the self magnetic field is longer in this regime but the peak amplitude is lower than in the case of moderate density materials, where the maximum magnetic field can exceed more than 2 times the laser field.

The maximum B-field, according to equation (3), with the currently available lasers and target materials is $\sim 2.5B_L$ if $R \approx 20$. This corresponds to $a_0 = 15$ and $n_0 = 200n_{cr}$ (for $\lambda_L = 400$ nm), which means $B_s \approx 1$ MT. In [6], fields greater than 1 MT was reported from a simulation with $R = 22$ and $B_L = 450$ kT. Using equation (3), and the parameters from that work, $B_s \approx 2.5B_L$ can be obtained, which is close to the simulation result.

3.2. Parallel nanorods

The maximum reachable magnetic field obtainable using current technology and available materials is just over 1 MT. This is over 4 orders of magnitudes greater than the fields produced by conventional devices (pulsed solenoids). However, the spatial extent of these extreme fields is very limited if only one nanorod is considered. Multiple nanorods grown on a plane metal surface result in the transversal magnetic field being the multiple of

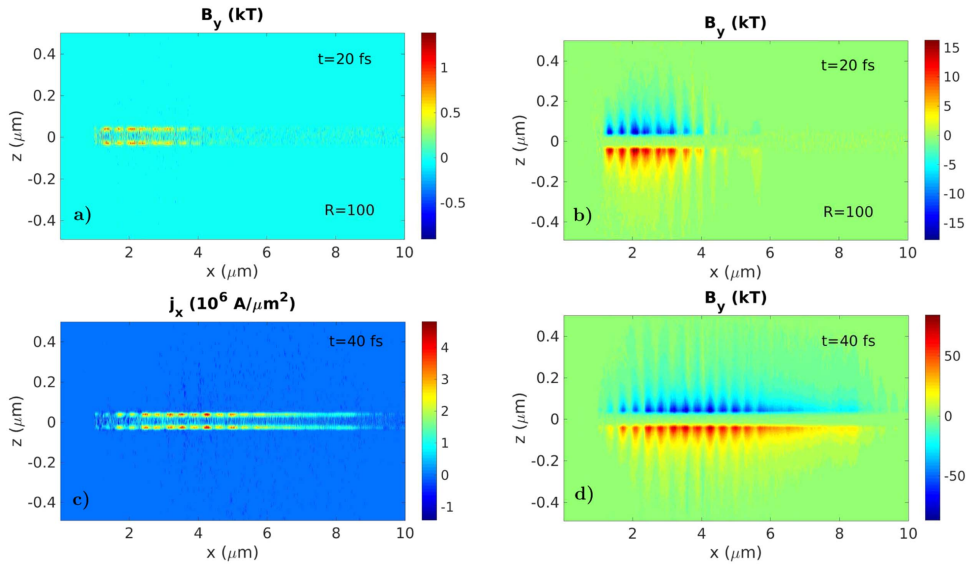

Figure 4. Longitudinal current density and azimuthal magnetic field cross sections at different time instances for a super heavy rod ($a_0 = 3.4$, $n_0 = 480 n_{cr}$).

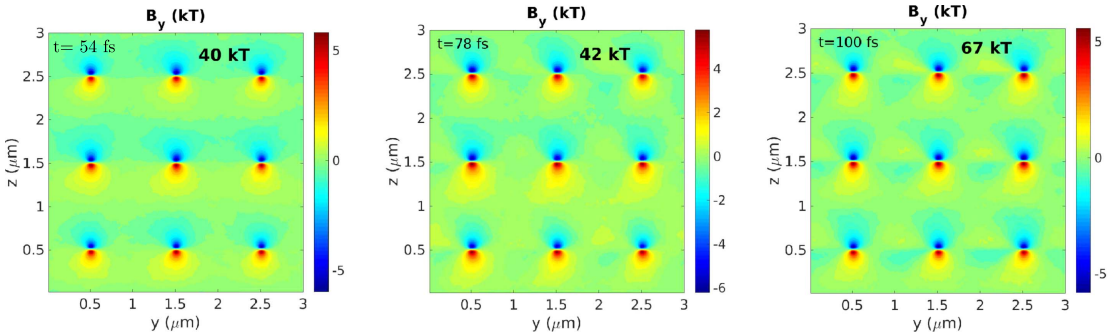

Figure 5. Induced magnetic field averaged along the x direction within the laser pulse at three different time instances. The values written in the top-right corners indicate the maximum magnetic field. Here $n_0 = 40 n_{cr}$, $a_0 = 13.67$, the lateral distance between nanorods is 1 μm and their diameter is the same as in section 3.1, 90 nm.

the single nanorod case if there is enough seperation between rods (figure 5). In the case of a nanorod array, the focal spot size of the laser pulse determines the number of nanorods taking part in the magnetic field generation. The use of multiple magnetic vortices requires the diameter of laser spot size to be much greater than the distance between nanorods, which is about one micron. The following parameters are needed for the generation of 1 MT field using $\lambda_L = 800$ nm wavelength laser: $n_0 = 400 n_{cr}$ and $a_0 = 36$, which corresponds to $I_L = 2.7 \times 10^{21}$ W cm^{-2}. This assumes a 30 μm^2 focal spot area and 30 fs pulse duration of full width at half maximum with a required pulse energy of ≈25 J, which can be provided by a currently available sub-petawatt class lasers.

The periodic structure of the transversal magnetic field observed in figure 5 enables the design of a micro-scale undulator, suitable to generate free electron laser (FEL) radiation with sub-nanometer wavelength. The relativistic electrons should be laterally inserted into the nanorod array, parallel with the magnetic field of the laser pulse. It has been shown that intense multi-keV photon burst can be produced in the direction of the laser propagation via interaction with nano-wires [12] but nano-wires are required as efficient synchrotron emissions are relatively long (>10 μm).

The current study shows that it is possible to generate long-lasting magnetic field with shorter nanorods if the electron density is high enough and the laser pulse is sufficiently long. One of the main draw-backs of the currently available FEL undulators is that the undulator wavelength (λ_u) can not be arbitrarily decreased due to the condition: $K = e\lambda_u B_0/(2\pi m_e c) > 1$, where B_0 is defined by the setup of the magnetic device and by the strength of permanent magnets. In the case of nano-rod targets $\lambda_u \approx 2$ μm and $B_0 \approx 50$ kT, yielding $K \approx 9$, which is sufficient for coupling between electron beam and radiation field. The short magnetic field period

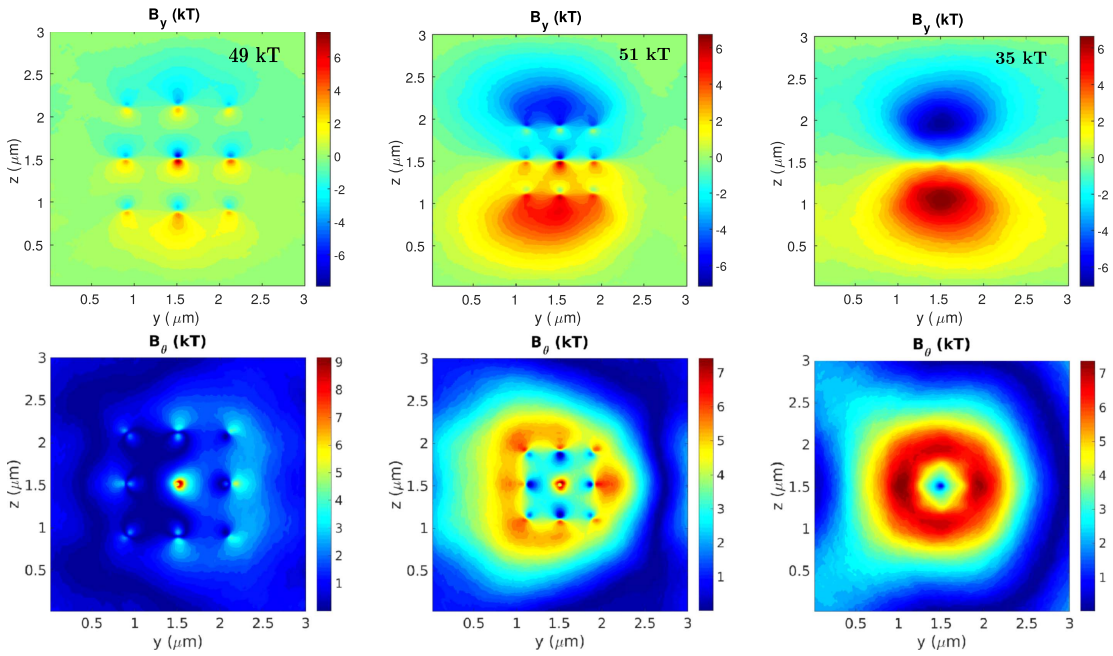

Figure 6. The same as in figure 5, but with converging nanorods. The azimuthal magnetic field is shown, calculated with respect to the central axis $(y_0, z_0) = (1.5\ \mu\text{m}, 1.5\ \mu\text{m})$.

allows the use of an electron beam with only 50 MeV ($\gamma = 100$) energy that can generate radiation within the water-window according to $\lambda_r = (\lambda_u/2\gamma^2)(1 + K^2/2) \approx 4$ nm. The challenge in realizing this setup lays in the short life-time of the generated magnetic field in a selected volume. Even if long laser pulses (pico-second duration) are used, the target has to be made from high Z material in order to slow down the radial expansion of nanorods and to maintain the internal return current.

3.3. Converging nanorods

It is possible to generate high magnetic field in a much larger volume if the nanorods are non-parallel, the distance between them decreases in the reference frame moving with the laser pulse. This arrangement can be realized by using a slightly bent flat foil (figure 1(b)). The B-field around rods merges into a single large azimuthal field as the rods converge, as shown in figure 6. The angle of these rods with respect to the x axis is 0.025 radian (1.4°), thus at the end the distance between the rods is only 0.25 μm, which is smaller than the excursion length of fast electrons in the laser field. The larger volume reduces the amplitude of the magnetic field but the spatial extension of the B-field can be controlled and compressed to increase its amplitude by using more surrounding nanorods or a cylindrical boundary.

In order to show that the produced azimuthal field has a donut shape, $B_\theta = B_z \cos(\alpha) - B_y \sin(\alpha)$, where $\alpha = \arctan[(z - z_0)/(y - y_0)]$ with $(y_0, z_0) = (1.5\ \mu\text{m}, 1.5\ \mu\text{m})$, is calculated and shown in the lower picture in figure 6. The magnetic field is initially generated around the individual nanorods in a small spot and later merges into a single azimuthal field. This field is generated by 9 nanorods which are now too close to each other to induce individual B-fields. The smaller distance means a stronger attracting $\mathbf{j} \times \mathbf{B}$ force, which leads to the merging of return currents flowing in the nanorods. If the value of R is not too high, the acting radial Lorentz force in this system can be stronger than the electrostatic force caused by the space-charge field of ions. Figure 7 shows that an average radial velocity of returning electrons can be observed. These point towards the center. This attraction between the return currents leads to the development of a single channel, which is wider than a single nanorod and induces a wider azimuthal magnetic field.

Figure 8 confirms the predictions of equation (2) as there is no significant change in the induced B-field amplitude with laser intensity and the field scales with $\sim n_0^{3/2}$, like the single nanorod cas. On the other hand the longitudinal profile of the B-field is self-similar if the ratio n_0/a_0 is constant, which follows from the similarity theorem [19]. The magnetic field along the rods is more uniform in the case of high density (blue line) because $R \approx 6$, while in the other two cases $R \approx 2$, and R also defines the spatial extension of the magnetic field, as described in section 3.1.

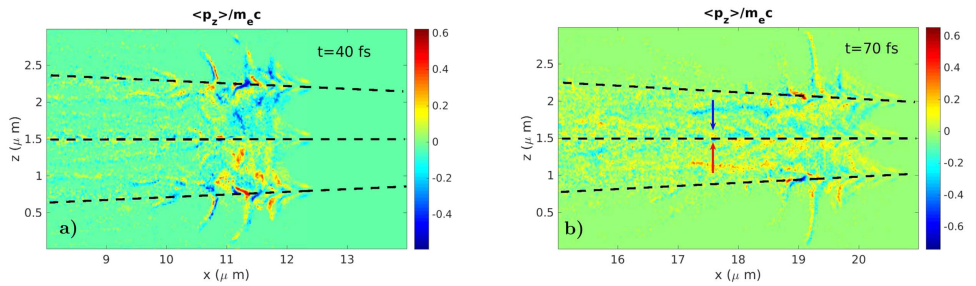

Figure 7. The averaged transversal momentum of slow electrons ($|p_z| < m_e c$) from the central cross-section of the simulation domain at two time instances. In this example $n_0 = 40 n_{cr}$, $a_0 = 42.8$ and the laser electric field is polarized in the y direction. The dashed lines show the original position of electrons.

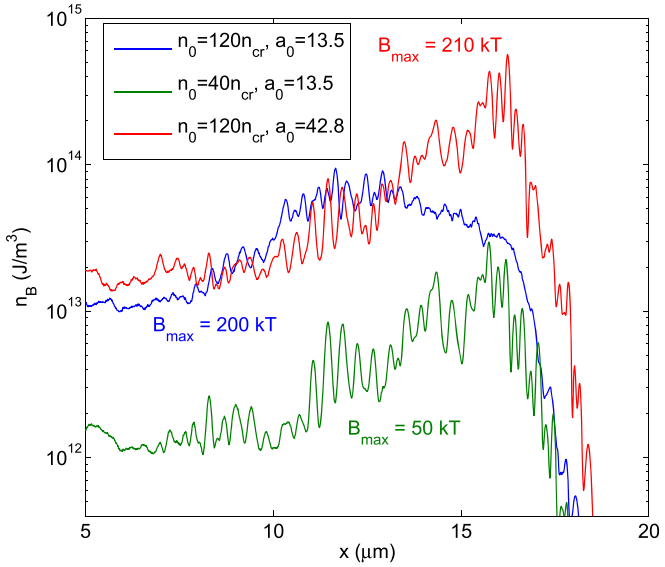

Figure 8. Transversally averaged energy density of B_y for different laser and plasma parameters.

4. Conclusions

A general scaling law for magnetic field strength achievable in the case of laser-nanorod interaction has been found using numerical simulations. A dimensionless parameter (R) has been used to uniquely describes the magnetic field generation and subsequently, three different regimes could be identified. The maximum field amplitude is about two times higher than the laser magnetic field and can be obtained for $R \approx 20$. A MT quasi static azimuthal magnetic field generation should be possible with the currently available, or the next-generation of multi-PW, laser sources, which could allow for realization of laboratory astrophysics or high energy physics experiments.

The spatial distribution of the magnetic field in such 2D array targets has been characterized and the rectangular periodic structure could be used in several micro-guiding devices, e.g., in micro-scale FEL. The very short undulator wavelength in principle could lead to the radiation of keV photons by using relatively low energy electron beams. It is also possible to generate one single azimuthal field in the focal volume of the laser pulse by using converging nanorods, where the magnetic fields around individual nanorods merge together into a single ring-like structure. The scalability of amplitude and tunability of spatial distribution should allow the application of nanorod targets in a wide area of laser-plasma physics.

Acknowledgments

The authors would like to thank the developer team of Tech-X Corporation for the help and support in solving the issues regarding the parallel performance of the simulation code (VSim). The high performance computer cluster was provided by the John Adams Institute (Oxford) supported by the UK STFC for JAI, grant ST/

J002011/1. The ELI-ALPS project (GOP-1.1.1.-12/B-2012-0001, GINOP-2.3.6-15-2015-00001) is supported by the European Union and co-financed by the European Regional Development Fund.

ORCID iDs

Zsolt Lécz https://orcid.org/0000-0001-5968-8012

References

[1] Fujioka *et al* 2013 KiloTesla magnetic field due to a capacitor-coil target driven by high power laser *Sci. Rep.* **3** 1170
[2] Tikhonchuk V T *et al* 2017 *Phys. Rev.* E **96** 023202
[3] Borghesi *et al* 1998 Megagauss magnetic field generation and plasma jet formation on solid targets irradiated by an ultraintense picosecond laser pulse *Phys. Rev. Lett.* **81** 112
[4] Tatarakis *et al* 2002 Measuring huge magnetic fields *Nature* **415** 280
[5] Sarri *et al* 2012 Dynamics of self-generated, large amplitude magnetic fields following high-intensity laser matter interaction *Phys. Rev. Lett.* **109** 205002
[6] Kaymak V, Pukhov A, Shlyaptsev V N and Rocca J J 2016 *Phys. Rev. Lett.* **117** 035004
[7] Jiang S *et al* 2016 *Phys. Rev. Lett.* **116** 085002
[8] Andreev A A and Platonov K Y 2014 *Opt. Spectrosc.* **117** 287–303
[9] Bargsten C *et al* 2017 *Sci. Adv.* **3** 1601558
[10] Purvis M A *et al* 2013 *Nat. Photon.* **7** 796–800
[11] Andreev A and Platonov K Y 2016 *Quantum Electron.* **46** 109–18
[12] Lécz Z and Andreev A 2017 *Phys. Plasmas* **24** 033113
[13] Davies J R 2006 *Laser Part. Beams* **24** 299–310
[14] Yoon P H and Davidson R C 1987 *Phys. Rev.* A **35** 2718
[15] Andreev A A and Platonov K Y 2013 *JETP Lett.* **98** 790–5
[16] Vshivkov V A, Naumova N M, Pegoraro F and Bulanov S V 1998 *Phys. Plasmas* **5** 2727
[17] Macchi A, Veghini S and Pegoraro F 2009 *Phys. Rev. Lett.* **103** 085003
[18] Nieter C and Cary J R 2004 Vorpal: a versatile plasma simulation code *J. Comput. Phys.* **196** 448–73
[19] Gordienko S and Pukhov A 2005 *Phys. Plasmas* **12** 043109